Published OnlineFirst November 24, 2009; DOI: 10.1158/1535-7163.MCT-09-0479

Combinatorial pharmacologic approaches target EZH2-mediated gene repression in breast cancer cells

Feng Sun,[1,2] Eli Chan,[2] Zhenlong Wu,[1] Xiaojing Yang,[1] Victor E. Marquez,[4] and Qiang Yu[1,3]

[1]Cancer Biology and Pharmacology, Genome Institute of Singapore, Agency for Science, Technology and Research (A*STAR), Singapore and Departments of [2]Pharmacy and [3]Physiology National University of Singapore, Singapore; and [4]Laboratory of Medicinal Chemistry, National Cancer Institute, Frederic, Maryland

Abstract

Polycomb protein EZH2-mediated gene silencing is implicated in breast tumorigenesis through methylation of histone H3 on Lysine 27 (H3K27). We have previously shown that S-adenosylhomocysteine hydrolase inhibitor 3-deazaneplanocin A can modulate histone methylation and disrupt EZH2 complex. Here, we used 3-deazaneplanocin A, together with other chromatin remodeling agents, as well as RNA interference–mediated EZH2 depletion, to probe the role of EZH2 in coordination with other epigenetic components in gene regulation in breast cancer cells. Through genome-wide gene expression analysis, coupled with extensive chromatin immunoprecipitation analysis of histone modifications, we have identified a variety of gene sets that are regulated either by EZH2 alone or through the coordinated action of EZH2 with HDAC and/or DNA methylation. We further found that tumor antigen *GAGEs* were regulated by distinct epigenetic mechanisms in a cell context–dependent manner, possibly reflecting mechanistic heterogeneity in breast cancer. Intriguingly, we found that EZH2 regulates a remarkable cohort of genes whose functions are highly enriched in immunoresponse and autocrine inflammation network, and that their transcriptional activation upon EZH2 perturbation is cancer specific, revealing a potential novel role of EZH2 in regulating cancer immunity. These findings show the complexity and diversity of epigenetic regulation in human cancer and underscore the importance for developing combinatorial pharmacologic approaches for effective epigenetic gene reactivation. [Mol Cancer Ther 2009;8(12):3191–202]

Received 6/2/09; revised 9/30/09; accepted 10/6/09; published OnlineFirst 11/24/09.

Grant support: A*Star grant GIS/06-711101 (Q. Yu). V. Marquez is supported by the intramural Research Program of the NIH, National Cancer Institute, Center for Cancer Research.

The costs of publication of this article were defrayed in part by the payment of page charges. This article must therefore be hereby marked *advertisement* in accordance with 18 U.S.C. Section 1734 solely to indicate this fact.

Note: Supplementary material for this article is available at Molecular Cancer Therapeutics Online (http://mct.aacrjournals.org/).

F. Sun and E. Chan contributed equally to this work.

Requests for reprints: Qiang Yu, Cancer Biology and Pharmacology, Genome Institute of Singapore, 60 Biopolis Street, #02-01 Genome, Singapore 138672. Phone: 65-6478-8127; Fax: 65-6478-9003. E-mail: yuq@gis.a-star.edu.sg

doi:10.1158/1535-7163.MCT-09-0479

Introduction

Abnormal epigenetic changes, including both DNA hypermethylation and histone modifications, have been implicated in cancer development (1, 2). Among various epigenetic modifying enzymes, the Polycomb repressor complex 2 (PRC2) is of particular importance because its key component EZH2, a histone methyltransferase specific for repressive H3K27 trimethylation (H3K27me3; refs. 3, 4), is often deregulated in human cancers (5–7). The role of EZH2-mediated gene silencing has been implicated in regulating cancer cell proliferation, invasion, and metastasis (7, 8). Moreover, increasing number of EZH2 or H3K27me3 target genes linked to important cancer pathways have been recently identified (9, 10). With continued efforts to identify EZH2 targets, it is expected that additional roles of EZH2 in carcinogenesis could be revealed.

Increasing evidences indicate that various silencing events are often interconnected and act in a coordinated manner (11, 12). It has been known that DNA methylation and methyl-CpG binding proteins are associated with histone deacetylation (13). In addition, EZH2 requires histone deacetylase (HDAC) for its gene silencing activity (7); it also recruits DNA methyltransferase (DNMT) to certain gene promoters to directly control DNA methylation (14). Therefore, a comprehensive unmasking of genes inactivated by the coordinated actions in cancer cells is highly required.

Since epigenetic modifications are reversible, they make attractive targets for therapeutic interventions. Genes silenced by DNA methylation in cancer can be reactivated by DNMT inhibitors such as 5-aza-2′-deoxycytidine (AZA; refs. 15, 16), or be synergistic with HDAC inhibitor, such as trichostatin A (TSA), which can facilitate the gene activation through reversing the repressed chromatin (17). In addition to the potential clinical use of these two classes of compounds, they are also widely used as research tools to identify genes silenced in cancer (18). Recent studies indicate that silenced tumor genes reactivated by DNMT inhibitors even with the aid of HDAC inhibitors do not return to an euchromatic chromatin state due to the retention of repressive histone marks, such as H3K27me3 (19, 20). These results highlight the need for perturbation of multiple epigenetic components for stable and complete gene reactivation.

3-Deazaneplanocin A (DZNep), a potent S-adenosylhomocysteine hydrolase inhibitor, was found to inhibit histone methylations. In particular, DZNep can effectively deplete the oncogenic PRC2 components EZH2, SUZ12, and EED,

Published OnlineFirst November 24, 2009; DOI: 10.1158/1535-7163.MCT-09-0479

as well as the associated H3K27me3, resulting in reactivation of PRC2-repressed target genes (21, 22). Moreover, it is synergistic with HDAC inhibitor to reprogram histone modifications, leading to robust gene reactivation (9). Given the frequent deregulation of EZH2 in human cancer, we thus hypothesized that the unique effects of DZNep on histone modifications make its use in combination with other chromatin remodeling agents an attractive approach for gene reactivation in cancer.

Here, we have used DZNep, and its combinations with other epigenetic drugs such as AZA or/and TSA, to characterize the various epigenetic events in breast cancer cells. Coupled with genetic depletion of EZH2, we have identified a comprehensive set of genes regulated by EZH2 in breast cancer through various epigenetic mechanisms. We further showed that EZH2 regulates a broad cohort of genes implicated in immunity and inflammation network, revealing a yet undisclosed link between EZH2 and cancer immunity. Our data indicate the cooperative nature of multiple epigenetic mechanisms in gene repression, which has imminent implications in epigenetic cancer therapy.

Materials and Methods

Cells and Drug Treatments

Cells (American Type Culture Collection) were maintained in DMEM supplemented with 10% fetal bovine serum. For drug treatment, cells were seeded the day before the drug treatment. Cells were treated with 2.5 μmol/L DZNep (National Cancer Institute) or 5 μmol/L AZA (Sigma) for 72 h, and TSA (Sigma) at 100 nmol/L for 24 h. For AZA treatment, the medium was replaced with freshly added AZA for every 24 h. For cotreatment of cells with DZNep and TSA, DZNep was added for 48 h followed by TSA for an additional 24 h.

RNA Interference

The siRNA targeting EZH2 and nontargeting control were purchased from 1st BASE Pte Ltd. as the following sequence: 5′-GACUCUGAAUGCAGUUGCU-3′. MCF-7 and SK-BR-3 cells were transfected with 100 nmol/L siRNA duplexes using Lipofectamine 2000 (Invitrogen) following the manufacturer's instructions.

Immunoblot Analysis

Cells were collected and lysed in radioimmunoprecipitation assay buffer as described previously (23). Equal amounts of protein (50 μg) were separated by SDS-PAGE and transferred onto polyvinylidene difluoride membranes (Millipore). Western blots were probed with the following antibodies: EZH2, EED, SUZ12, H3K9me3, H3K27me3, H3K9/K14ac, and H3K4me3 were purchased from Upstate Biotechnology; H4K20me3 was from Abcam; Histone H3 (3H1) and actin was from Cell Signaling; and DNMT1 and DNMT3B were from Alexis Biochemicals.

Microarray Analysis

Total RNA was isolated from cells using the RNAeasy Mini kit (Qiagen). The microarray hybridization was done using the Illumina Gene Expression BeadChip (Illumina). Data visualization, clustering, and differential analysis were carried out with BeadStudio software (Illumina) and GeneSpring GX program, 7.3. (Silicon Genetics). The differentially expressed genes between any pair groups were defined as a >3-fold change in the mean gene expression between two groups and converted to "expression ratio" by dividing each value by the mean signal value of that gene in the control group. Three separate experiments were implemented to enhance the reliability of the gene expression data. The genes were grouped according to their functional characteristics through the Gene Ontology database. Genes were clustered and displayed using average linkage clustering. The microarray data have been submitted to the GEO public database (accession number GSE17589).

Reverse Transcription-PCR and Quantitative Real-time PCR

One microgram of total RNA from each sample was subjected to PCR using One Step reverse transcription-PCR kit (Clontech) according to the manufacturer's protocol. The PCR product was separated and photographed on a 2.0% agarose gel containing ethidium bromide. Quantitative Real-time PCR (qRT-PCR) was done on a PRISM 7900 Sequence Detection System (Applied Biosystems) using Taqman probes (Applied Biosystems). Samples were normalized to the levels of 18S rRNA. The primer sequences and the key parameters used are included in the Supplementary Table S1. The average values for qRT-PCR were from three experiments.

DNA Methylation Analysis

DNA methylation status at the CpG island was determined by PCR analysis after bisulfited modification and followed by methylation-specific PCR (MSP) or Bisulfite genomic sequencing (BGS; ref. 24). Briefly, for MSP, Genomic DNA extracted from MCF-7, SK-BR-3, BT-474, and MCF10A cells was treated with sodium bisulfite using the EZ DNA Methylation-Gold kit (ZYMO) overnight. The bisulfite-treated DNA was amplified with either a methylation-specific or unmethylation-specific primer set. For BGS, bisulfite-treated DNA was amplified using a BGS primer set. PCR products were used for TOPO Cloning (Invitrogen) and followed with sequencing. The primer sequences and the key parameters are available in Supplementary Table S1.

Chromatin Immunoprecipitation Assays

Chromatin immunoprecipitation (ChIP) asays were done as described previously (25). The immunoprecipitated DNA was quantitated by qRT-PCR using S probes (Applied Biosystems). Primer set was chosen to amplify approximately 100 to 200 bp around the indicated region. We used the following antibodies in the ChIP study: H3K27me3, H3K9/14ac, and H3K4me3 were purchased from Upstate Biotechnology; and H3K9me3 was from Abcam and EZH2 from Active motif. The enrichments of these histone marks were quantitated relative to the input amount. To compare the two pools of DNA materials, a further normalization of the $^{\Delta}$Ct values were against a region with low background enrichment. The sequences of the PCR primers are shown in Supplementary Table S1. Values were calculated as the average from two independent experiments. The value that is

Published OnlineFirst November 24, 2009; DOI: 10.1158/1535-7163.MCT-09-0479

<2 is classified as the baseline. Two-sided Student's *t* test was used ($P < 0.05$).

Results

The Effects of DZNep in Combination with Other Epigenetic Drugs on Histone Modifications

Given the heterogeneity and complexity of epigenetic mechanisms in gene inactivation, we postulated that combinatorial epigenetic drug treatment targeting distinct epigenetic processes might act in synergy to give rise to maximal gene reactivation. We have previously shown that DZNep inhibits histone methylations and in particular inhibits PRC2 complex and associated H3K27me3 in breast cancer cells (22). In this study, we wished to determine the effect of DZNep in combination with other epigenetic drugs on histone modifications. Specifically, we treated breast cancer MCF-7 cells with DZNep, AZA, and TSA, alone or in various combinations (seven treatment conditions).

We first examined the effects of such treatments on histone modifications and the associated histone-modifying enzymes by Western blotting. As previously shown, DZNep treatment resulted in remarkable reduction of PRC2 components SUZ12, EZH2, EED, and associated H3K27me3 but had no effect on H3K9me3 and H3K9/14 acetylation (H3K9/14ac; ref. 22); it also had no effect on DNMT1 and DNMT3b (Fig. 1A). Of significant notice, DZNep and TSA combination induced a robust increase in H3K9/14ac, which was nearly undetectable in cells treated with TSA alone, indicating a strong synergistic effect of DZNep and TSA on histone acetylation. By contrast, DZNep and AZA combination did not give rise to the same effect. DZNep also inhibited H3K4me3, but this inhibition was reversed by its combination with TSA. On the other hand, AZA depleted DNMTs effectively as previously reported (26), but had little effect on the above histone modifications. Thus, treatment of MCF-7 cells with DZNep and TSA induced marked changes in histone modifications: it reduced the repressive histone mark H3K27me3 but increased or at least maintained active marks H3K9/14ac and H3K4me3.

It is especially intriguing that combination of DZNep and TSA induced a robust augment of histone H3K9/14ac.

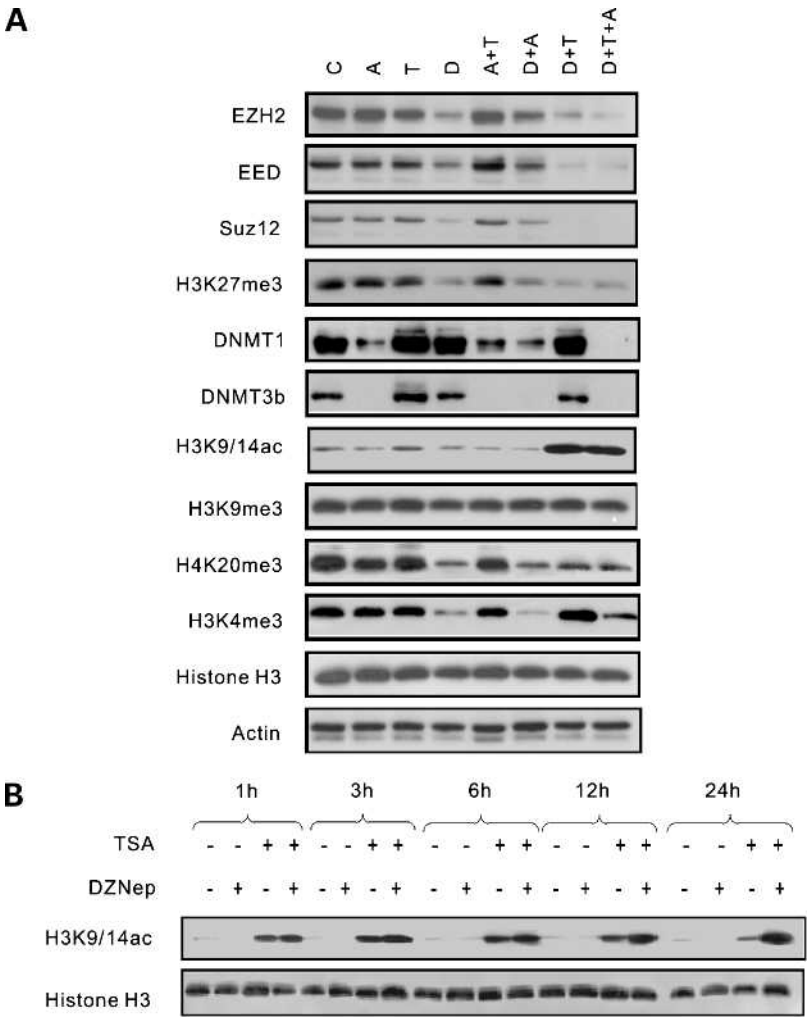

Figure 1. Changes of histone modifications in response to different drug treatments. **A,** Western blot results show the changes of PRC2 proteins, DNMTs, and indicated histone modifications in MCF-7 cells after treatment with DZNep (*D*), TSA (*T*), and AZA (*A*) alone or in various combinations. β-Actin was used as a loading control. **B,** Western blot results show the changes of H3K9/14ac at indicated time points following the treatment of DZNep (2.5 μmol/L), TSA (100 nmol/L), or both in MCF-7 cells.

Published OnlineFirst November 24, 2009; DOI: 10.1158/1535-7163.MCT-09-0479

Given the dynamic nature of histone acetylation, we next set to examine the changes of H3K9/14ac over time following the above drug treatments. Figure 1B illustrates the time course of H3K9/14ac induced by TSA in the presence or absence of DZNep. TSA alone induced strong acetylation as early as 1 hour, which gradually returned to the baseline at 24 hours. In the presence of DZNep, TSA-induced H3K9/14ac remained elevated overtime, indicating that DZNep treatment facilitates histone acetylation for a prolonged period of time.

The results indicate that combination of DZNep and TSA causes a global reprogramming of histone modifications. The magnitude of the effect observed on general histone profiles further suggests that it might be widespread throughout the genome, which is expected to have profound effect on global gene expression as described below.

Differential Gene Expression Response Patterns to Various Drug Combination Treatments

To determine the global gene expression changes following the above epigenetic drug treatments, we performed microarray analysis using Illumina BeadArray system in MCF-7 cells exposed to above seven treatment conditions. In total, we identified 657 genes that were upregulated by AZA alone (using 3-fold cut off, $P < 0.05$), indicating that expression of these genes might be repressed by DNA methylation. We also identified 372 genes upregulated by DZNep alone or in combination with other agents (using 3-fold cut off, $P < 0.05$), indicating that repression of this gene set might be associated with histone methylations (thereafter called DZNep-related genes). Comparing the two gene lists by Venn diagram revealed an overlap of only 64 genes, indicating that the two silencing events regulate distinct sets of genes (Fig. 2A). This finding agrees with the recent genome-wide analyses showing that most genes enriched at H3K27me3 are not targets of DNA methylation and *vice versa* (10, 27).

Of 372 DZNep-related genes are those strongly upregulated by DZNep alone ($n = 181$) or in synergy with TSA ($n = 177$; Fig. 2A). Two sets of genes were divided according to whether gene expression (normalized) induced by DZNep plus TSA is >2-fold of that of DZNep alone. Among 372 DZNep-related genes, 64 genes also showed induction by AZA treatment. Of these 64 genes, 28 genes were mainly upregulated by DZNep and 22 by DZNep plus TSA. The remaining 14 genes showed response to AZA-related treatment but not to DZNep or DZNep plus TSA. Because epigenetic events associated with AZA and TSA have been previously investigated in large numbers of literatures (28–30), we chose to focus on 372 DZNep-related genes that may reveal novel insights into distinct models of epigenetic regulation involving histone methylations.

Gene cluster analysis further presents three patterns of DZNep-related genes. The first cluster (cluster I, D+T pattern, $n = 177$) in general shows a robust response to DZNep plus TSA treatment (34.8-fold induction) compared with the single treatment. By contrast, other combination treatments, such as DZNep plus AZA (D+A) or AZA plus TSA (A+T) failed to give such an effect (Supplementary Table S2; Fig. 2B). Therefore, the expression of these genes such as *TNF* and *CCL2* (Fig. 2C) appeared to be mainly regulated by a synergistic effect of both histone methylation and deacetylation, but not DNA methylation. Notably, many genes in this cluster are cytokines and chemokines such as *TNF, IL8*, and *CXCL2* that are implicated in a wide range of biological disorders, including tumorigenesis.

The second cluster (cluster II, D pattern, $n = 181$) appears to be sensitive to DZNep treatment alone (24.0-fold induction) and further combination with other agents did not yield further induction. Many of these genes, such as *IGFBP3, KRT17*, and *FBXO32* (Fig. 2C), have been identified as PRC2 targets in our previous study (22). For these genes, histone methylation seems to be the primary mechanism responsible for their silencing, and neither DNA methylation nor histone deacetylation seems to be important.

The third cluster (cluster III, D+T+A pattern, $n = 14$) represents a small gene set that were responsive to AZA (18-fold induction), but not to DZNep, TSA, or DZNep plus TSA, indicating that DNA methylation is the dominant mechanism responsible for their silencing. In addition, combination of AZA with TSA and DZNep further enhanced their expression (80.2-fold), indicating that histone modifications robustly coordinate with DNA methylation to cause their silencing. Included in this cluster were members of a family of genes encoding *GAGE*- and *MAGE*-type tumor antigens, which have been previously shown to be silenced by DNA hypermethylation (26, 31). Restored expression of these tumor antigens in cancer by DNA demethylating agent has been implicated in tumor immunotherapy. Hence, as described above, combination treatment targeting multiple epigenetic processes is able to yield maximal induction of these tumor antigens. qRT-PCR analysis of 12 genes selected to represent each cluster validated the Illumina microarray data (Supplementary Fig. S1).

Collectively, based on the distinct gene expression response patterns to different epigenetic drug combination treatments, we are able to predict the primary mechanism by which the affected genes are epigenetically repressed. Among various drug combinations, DZNep plus TSA, or further with AZA seem to be of high interest as they may represent a highly synergistic model of actions among various epigenetic events in gene silencing.

Chromatin Modifications of Selected Gene Loci Reflecting Associated Drug Response

GAGE2, TNF, and *CCL2* represent gene cluster I and III that are regulated by coordinated actions of histone modifications, whereas *KRT17* represents gene cluster II that is repressed only by histone methylation. We first used MSP to determine their promoter DNA methylation status in MCF-7 cells. MSP analysis revealed methylated promoter of *GAGE2*, whereas *KRT17, TNF*, and *CCL2* promoters were largely free of DNA methylation (Fig. 3A).

We next used ChIP coupled with qRT-PCR to characterize potentially involved histone marks, including the repressive marks H3K27me3, H3K9me3, and EZH2 as well as the activating marks H3K4me3 and H3K9/14ac. To this end, we have scanned ~5 kb genomic region surrounding the

Published OnlineFirst November 24, 2009; DOI: 10.1158/1535-7163.MCT-09-0479

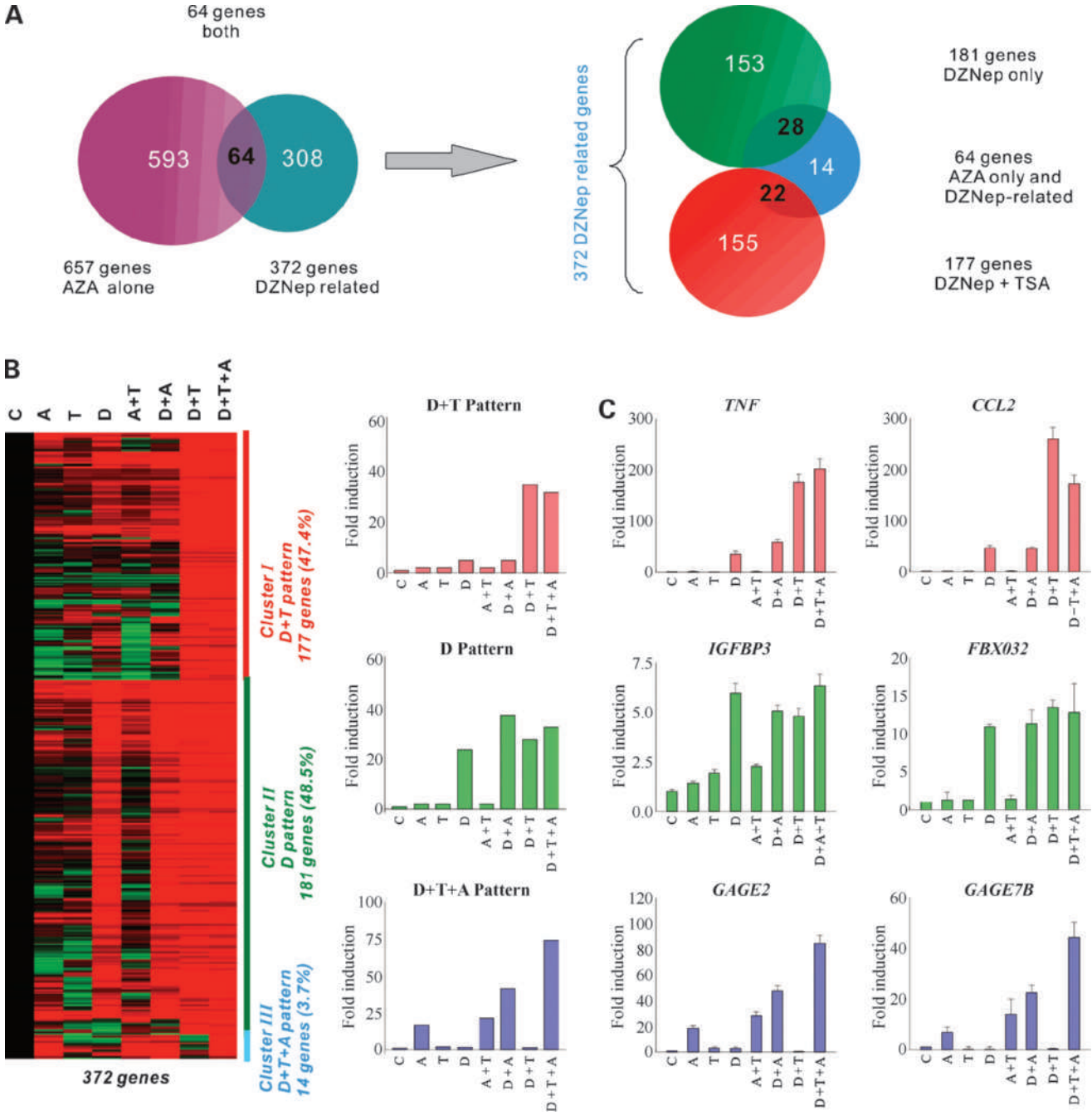

Figure 2. Distinct gene expression response profiles to different drug treatments. **A,** the left Venn diagram shows 657 and 372 genes in MCF-7 cells that were upregulated for ≥3-fold by AZA alone and DZNep-related treatments, respectively, with 64 genes showing the overlap between the two groups. The right Venn diagram shows the breakdown of 372 DZNep-related genes, including 181 genes induced by DZNep alone, 64 genes induced by both AZA and DZNep, and 177 genes induced by combination of DZNep with TSA. **B,** hierarchical clustering showing the expression profiles of 372 DZNep-related genes in three distinct patterns: DZNep plus TSA sensitive (cluster I, D + T pattern), DZNep sensitive (cluster II, D pattern), and triple combination sensitive (cluster III, D + T + A pattern). Shown on the right side are the averaged response patterns of each cluster following the indicated drug treatments. **C,** expression patterns of selected genes representing each cluster (*columns,* mean of triplicate measurement; *bars,* SD). *TNF* and *CCL2* (*D + T pattern*), *IGFBP3* and *FBXO32* (*D pattern*), *GAGE2* and *GAGE7B* (*D + T + A pattern*).

transcription start site (TSS) of *GAGE2, KRT17, TNF,* and *CCL2* in MCF-7 cells. ChIP results detected abundant EZH2 and H3K27me3 enrichment in a 200 to 800 bp region downstream of the TSS of all four genes (Fig. 3B). This result is consistent with the several recent genome-wide studies showing that a large portion of H3K27me3 is detected in the proximal downstream region of the TSS in both cancer and embryonic stem cells (32, 33). Coupled with no

Published OnlineFirst November 24, 2009; DOI: 10.1158/1535-7163.MCT-09-0479

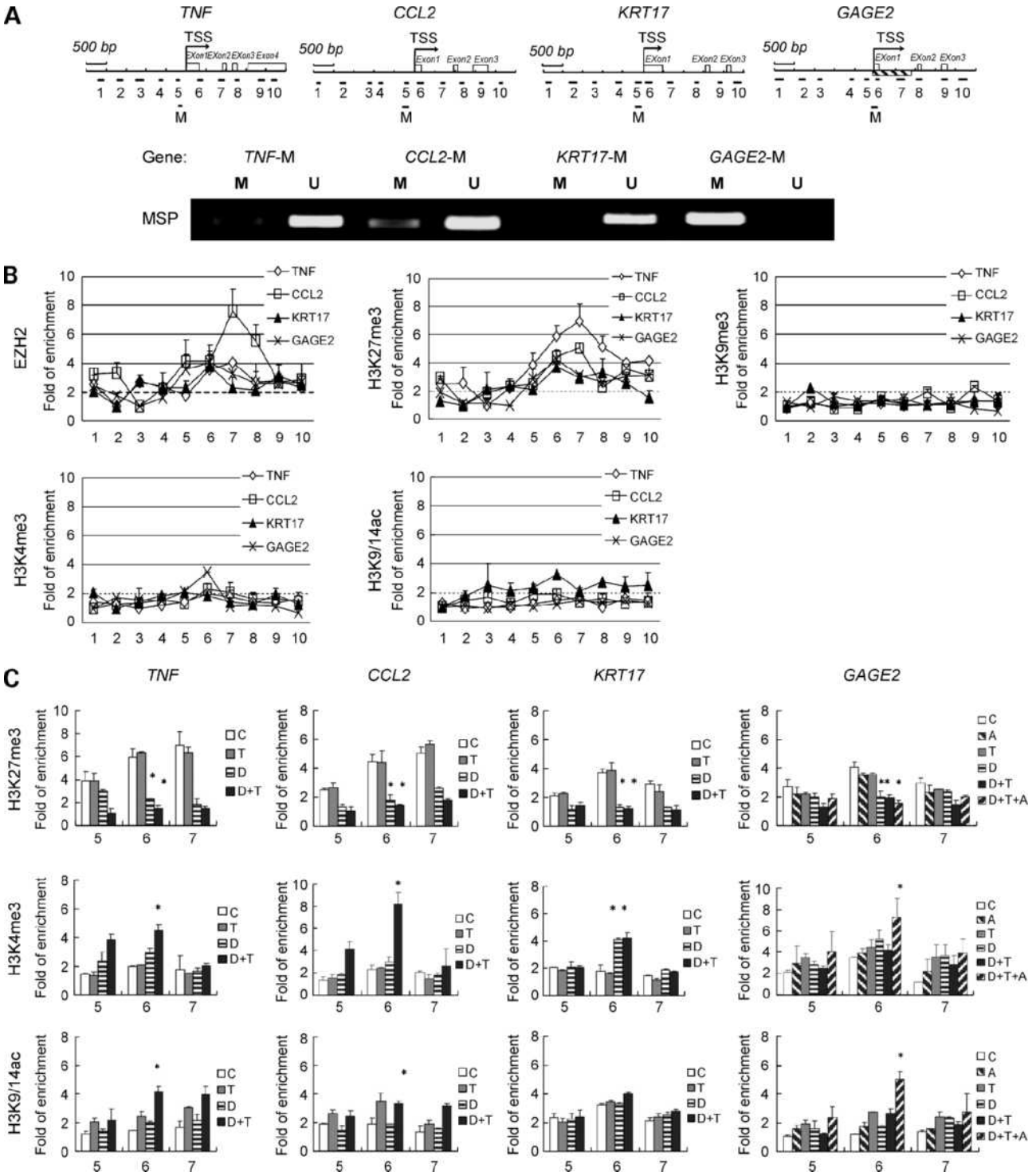

Figure 3. Chromatin modifications in *TNF, CCL2, KRT17*, and *GAGE2*. **A,** genomic DNA fragments covering the −2.5 to +2.5 kb region for *TNF, CCL2, KRT17*, and *GAGE2* relative to the TSS for PCR analysis are indicated with numbers. *Hatched bar below the line,* CpG islands. *M,* the examined PCR regions for methylation analysis. MSP analysis of *TNF, CCL2, KRT17*, and *GAGE2* promoters in MCF-7 cells indicates hypermethylated *GAGE2* and largely unmethylated *TNF, CCL2*, and *KRT17*. **B,** EZH2 and histone marks (H3K27me3, H3K4me3, H3K9/14ac, and H3K9me3) at the each gene locus in MCF-7 cells. ChIP assays were done using antibodies against the indicated histone modifications and analyzed by qRT-PCR. The values represent the normalized enrichments against the background region. The relative enrichments (bound/input; *points,* mean of duplicate measurement; *bars,* SD) encompassing the indicated regions are shown for each histone mark at each gene locus. The value that is 2 is classified as the baseline (*dashed lines*). **C,** ChIP analysis indicates the changes of histone marks (H3K27me3, H3K4me3, and H3K9/14ac) at four gene loci in MCF-7 cells after indicated drug treatments. *Columns,* mean of two independent experiments; *bars,* SD. *, $P < 0.05$. The numbers along the *X*-axis indicate the ChIP-PCR positions as in **A**.

Published OnlineFirst November 24, 2009; DOI: 10.1158/1535-7163.MCT-09-0479

H3K9me3 mark being detected, these results suggest that the transcription of these four genes is regulated under the EZH2-H3K27me3. On the other hand, H3K9/14ac was not found to be enriched in *TNF, CCL2*, and *GAGE2*, although more in *KRT17*. Of notice, H3K4me3 was detected near the *GAGE2* TSS in MCF-7 cells, suggesting that the *GAGE2* promoter is simultaneously modified by both repressive and activating histone methylation in these cells. Such bivalent histone states have been previously shown to correlate with genes transcribed at low levels (5, 33). Taken together, the high levels of repressive EZH2-H3K27me3 and low levels of activating H3K4me3 at these genes are consistent with their repressed expression in MCF-7 cells, although H3K9/14ac might be responsible for the difference of gene expression response between cluster I and cluster II.

ChIP analysis of drug-treated samples indicated that H3K27me3 at *TNF, CCL2*, and *KRT17* was markedly reduced by DZNep with or without TSA (Fig. 3C). In contrast, H3K4me3 and H3K9/14ac were only induced in cells treated with DZNep plus TSA at *TNF* or *CCL2*. This result is consistent with the strong induction of the above two genes by DZNep plus TSA but less by DZNep or TSA alone. The data also suggest that for class I genes (*TNF* and *CCL2*) the inhibition of H3K27me3 alone is not sufficient for their full reactivation. In such case, perturbation of both H3K27me3 and HDAC seems to be required for an effective alleviation of their repression. In contrast, as for cluster II genes (*KRT17*), the inhibition of H3K27me3 by DZNep alone was sufficient for their reactivation and addition of TSA did not seem to further increase H3K4me3 and H3K9/14ac. Furthermore, with respect to cluster III genes (*GAGE2*), although DZNep or DZNep plus TSA can effectively alleviate H3K27me3, an induction of H3K4me3 or H3K9/14ac was only found in cells treated with the triple combination. Therefore, coupled with gene expression pattern of these three clusters, the collateral effects of inhibition of H3K27me3 and increase in H3K4me3/H3K9/14ac seem to be required for an efficient induction of affected target gene expression.

Mechanistic Heterogeneity of Epigenetic Regulation of Tumor Antigen *GAGE*s in Breast Cancer

Members of *GAGE* family are cancer antigens whose expression is restricted to immunoprivileged normal tissues and different types of cancers, which make them attractive candidates for cancer-specific immunotherapy (34, 35). As shown above, *GAGEs* are silenced in MCF-7 cells, thus making the immunology-based approach unlikely. Given breast cancer is characterized by its cellular heterogeneity, we further extended our analysis to other breast cancer cell lines to determine whether *GAGEs* are expressed differentially in these cells. Screening our Illumina gene expression database of breast cancer cell lines repository revealed that *GAGEs* in various breast cancer cell lines are generally expressed in three different levels. As shown in Table 1, although *GAGEs* showed a silenced expression in MCF-7 cells with values from -7 to 10.3, they were basally expressed in SK-BR-3 cells (344.0–450.1) and highly in BT-474 cells (15,706.7–22,883.3). Therefore, these three cell lines represent three distinct models of regulation of *GAGEs* expression in breast cancer.

Table 1. The different gene expression levels of *GAGE* family members in three representative breast cancer cell lines: MCF-7, SK-BR-3, and BT-474 cells

	MCF-7	SK-BR-3	BT-474
GAGE2	−0.9	388.4	16,895.8
GAGE4	−5.5	400.7	16,808.2
GAGE5	6.4	450.1	15,706.7
GAGE6	10.3	344.0	22,883.3
GAGE7B	1.2	392.8	16,305.6
GAGE8	−7	415.8	16,840.7

NOTE: Data are raw expression values in Illumina Beadarray.

As the first step to understand the epigenetic mechanism underlying this difference, we examined the methylation status of the *GAGE2* promoter in these cells. The BGS analysis indicates that *GAGE2* promoter was unmethylated in both SK-BR-3 cells and BT-474 cells, as opposed to methylated in MCF-7 cells (Supplementary Fig. S2). This finding suggests that although the silenced expression of *GAGE2* in MCF-7 is linked to DNA methylation, the low expression of *GAGE2* in SK-BR-3 cells is associated with alternative mechanisms.

ChIP analysis indicates that H3K27me3 was highly enriched in SK-BR-3 cells, less enriched in MCF-7, and in lowest level in BT-474 cells (Fig. 4A). H3K4me3, on the other hand, was highly enriched in BT-474 cells, modestly in SK-BR-3 cells, and low in MCF-7 cells, corresponding well with different expression levels of *GAGE2* in these cell lines. Thus, *GAGE2* in SK-BR-3 cells displays a bivalent chromatin as it carries both H3K27me3 and H3K4me3, consistent with its basal expression in this cell line. In contrast, *GAGE2* in MCF-7 cells, whose expression was scarcely detected, is marked with both DNA methylation and a bivalent histone modification. In addition, H3K9me3 was not enriched in *GAGE2* in all the three cell lines, suggesting that this repressive mark is not important for *GAGE2* repression in cancer cells.

Consistent with above chromatin structures, DZNep plus TSA treatment resulted in a strong synergistic induction of *GAGEs* in SK-BR-3 cells (Supplementary Table S3; Fig. 4B), although little in MCF-7 cells carrying promoter methylated *GAGE2*. In BT-474 cells, *GAGEs* were highly expressed and thus only showed modest response to DZNep plus TSA.

As shown in Fig. 4C, DZNep plus TSA treatment of SK-BR-3 cells resulted in a dramatic decrease in H3K27me3, but concomitantly increases in H3K4me3 and H3K9/14ac, whereas neither TSA nor DZNep alone increased H3K4me3. Collectively, these results suggest that the strong induction of *GAGE2* in SK-BR-3 cells following DZNep plus TSA treatment reflects synergistic effects of the two epigenetic agents on histone modifications (D+T pattern).

As shown above, *GAGE2* silencing in MCF-7 cells is associated with both DNA methylation and histone methylation, and a triple combination treatment is required for a maximal reactivation. Pharmacologic induction of tumor antigens

Published OnlineFirst November 24, 2009; DOI: 10.1158/1535-7163.MCT-09-0479

such as GAGEs in cancer cells may provide a benefit to prime the cancer cells for immunnotherapy. One concern for such a treatment is that it might also lead to the *GAGE2* induction in normal cells. However, we found that the triple drug combination treatment did not induce *GAGE2* in MCF10A cells (Supplementary Fig. S3A). In MCF10A cells, *GAGE2* promoter was also hypermethylated (Supplementary Fig. S3B), without detectable H3K27me3 (Supplementary Fig. S3C). Instead, a strong H3K9me3 was detected. This finding suggests that the enrichment of H3K27me3 at *GAGE2* locus may be a cancer-specific event, which explains why MCF-7 cells but not MCF10A cells showed reactivation of GAGEs by DZNep-related combination treatment. The silencing of *GAGE2* in MCF10A cells seems to be related to DNA methylation and H3K9me3 that are resistant to DZNep-related treatment.

Functional Determination of EZH2 as a Crucial Regulator of *GAGE2* Expression

Having shown the effect of DZNep on *GAGE2* expression, we next set out to determine whether EZH2 knockdown would give rise to a similar effect on *GAGE2* expression in MCF-7 and SK-BR-3 cells, alone or in combination with other epigenetic drugs. As shown in Fig. 5A, both cell lines treated with EZH2 siRNA displayed a marked decrease in EZH2 expression and a corresponding decrease in H3K27me3. Further treatment with AZA plus TSA in MCF-7 cells or TSA alone in SK-BR-3 cells resulted in remarkable increase in H3K9/14ac. This effect mimicked the one of DZNep in synergy with TSA on the above histone modifications as previously shown in Fig. 1A.

As anticipated, EZH2 knockdown, in combination with AZA plus TSA, induced strong re-expression of *GAGE2* in MCF-7 cells (Fig. 5B), resembling the effect induced by the triple combination treatment. Likewise, EZH2 knockdown in SK-BR-3 cells resulted in robust induction of *GAGE2* in the presence of TSA, similar to that induced by DZNep plus TSA. Taken together, these results confirm a crucial role of EZH2 in repressing *GAGE2* in breast cancer cells, either through coordination with both histone deacetylation and

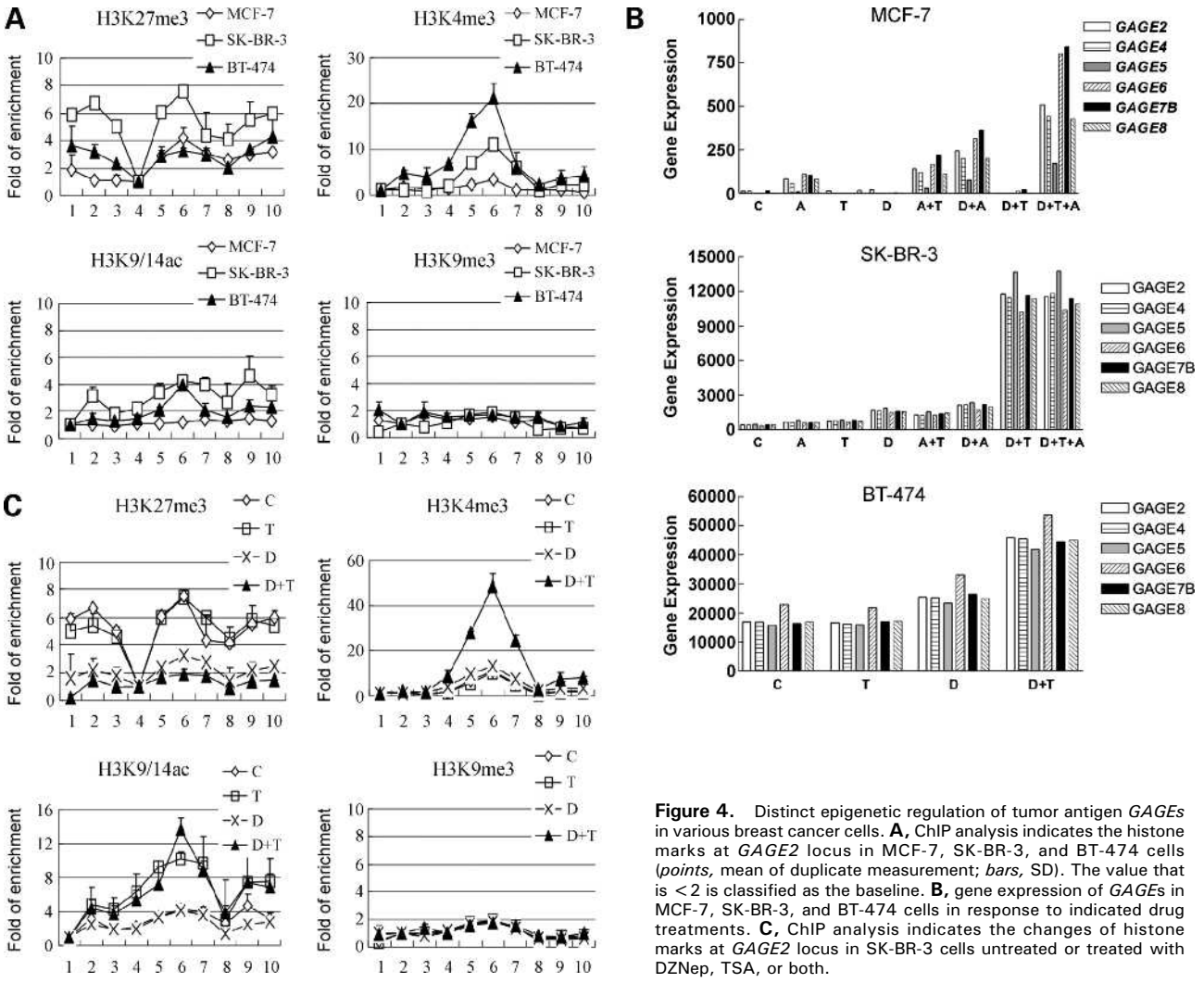

Figure 4. Distinct epigenetic regulation of tumor antigen *GAGEs* in various breast cancer cells. **A,** ChIP analysis indicates the histone marks at *GAGE2* locus in MCF-7, SK-BR-3, and BT-474 cells (*points,* mean of duplicate measurement; *bars,* SD). The value that is <2 is classified as the baseline. **B,** gene expression of *GAGE*s in MCF-7, SK-BR-3, and BT-474 cells in response to indicated drug treatments. **C,** ChIP analysis indicates the changes of histone marks at *GAGE2* locus in SK-BR-3 cells untreated or treated with DZNep, TSA, or both.

Published OnlineFirst November 24, 2009; DOI: 10.1158/1535-7163.MCT-09-0479

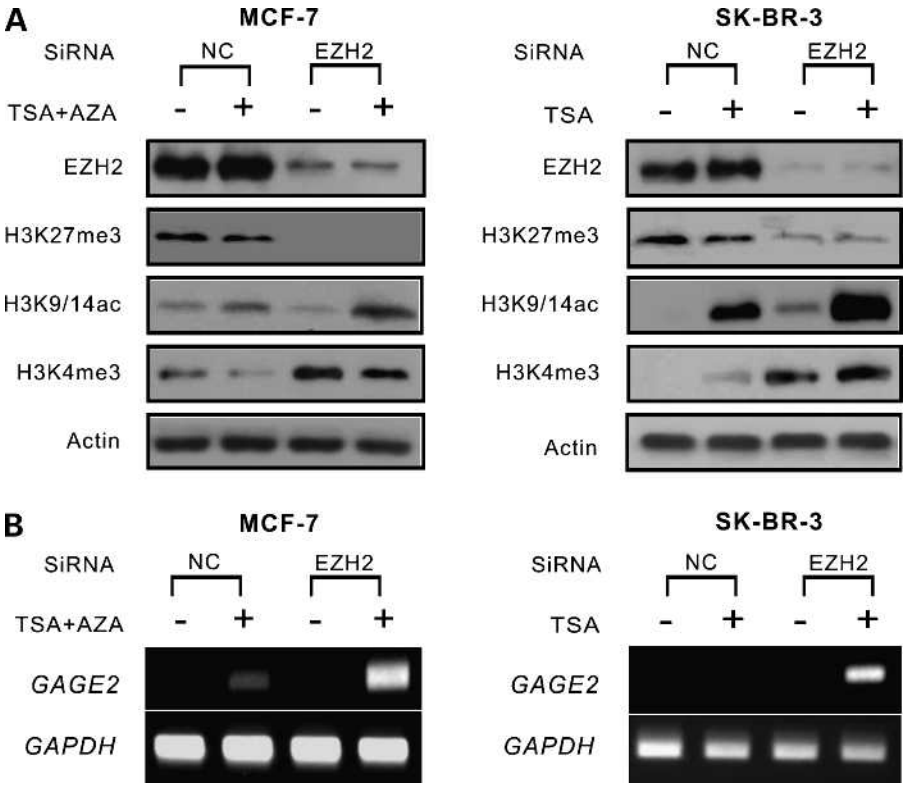

Figure 5. EZH2 is a crucial regulator of *GAGE2* expression. **A,** Western blotting analysis showing the changes of EZH2, H3K27me3, H3K9/14ac, and H3K4me3 protein levels. MCF-7 cells were treated with nontargeting control (*NC*) or EZH2 siRNA for 24 h, followed by treatment with TSA plus AZA for additional 24 h. SK-BR-3 cells were treated with NC or EZH2 siRNA for 24 h, followed by TSA treatment for additional 24 h. **B,** reverse transcription-PCR analysis of *GAGE2* mRNA levels in MCF-7 and SK-BR-3 cells treated as above. *GAPDH* served as a loading control.

DNA methylation in MCF-7 cells or histone deacetylation only in SK-BR-3 cells.

EZH2-H3K27me3 Regulates the Inflammation Network That Is Activated by DZNep Alone or in Synergy with TSA in MCF-7 Cells

In MCF-7 cells, 96% of 372 DZNep-related genes are those induced by DZNep alone or in combination with TSA (Fig. 2B). To systematically identify EZH2-repressed targets that can be reactivated by above drug treatments, we performed microarray analysis in MCF-7 cells and identified 340 genes that were induced by either EZH2 siRNA alone or in combination with TSA (3-fold cut off, $P < 0.05$). Further comparing them with the gene sets induced by DZNep alone or together with TSA gives rise to a common set of 213 genes, which represents EZH2-repressed gene targets that are reactivated by the above drug treatments.

To identify EZH2-related gene response that may represent a cancer-specific event, we further compared the above gene list with that in MCF10A cells under the same drug treatments. This analysis resulted in the identification of a set of 148 genes that are strongly induced in MCF-7 cells by EZH2 siRNA or DZNep with or without TSA but not in MCF10A cells (Fig. 6A). Thus, we have uncovered a cohort of 148 genes repressed by EZH2 that can be reactivated by DZNep or DZNep plus TSA treatment in a potential cancer-specific manner. Furthermore, this set of genes was also similarly induced in SK-BR-3 cells (Supplementary Fig. S4), suggesting that EZH2-mediated repression of these genes also occurred in other breast cancer cell lines.

Gene Ontology analysis revealed that the 148 gene set covers a broad range of functional categories (Fig. 6B). Of significant notice, a set of 58 genes functioning in inflammation and immune response was remarkably enriched (39%; Supplementary Table S4). This is significantly higher than the 11.9% (1,510) of inflammation-related genes out of all genes in the array (21,007; $P < 0.01$, χ^2 test). The data suggest a potential role of EZH2 in the regulation of immune response in breast cancer cells. These genes include cytokines and chemokines such as *TNF*, *IL8*, *CCL2*, *CCL20*, and *CXCL2*, etc. Furthermore, consistent with the cancer-specific induction following EZH2 perturbation, ChIP analysis detected the enrichment of EZH2 and H3K27me3 in *TNF* and *CCL2* in MCF-7 cells but not in MCF10A cells (Fig. 6C), supporting that EZH2-H3K27me3 may regulate a wide range of gene involved in inflammation network in breast cancer cells.

Discussion

DZNep is a potent inhibitor of S-adenosylhomocysteine hydrolase (ref. 36). Although it seems to be a general methyl-donor inhibitor, DZNep had a minimal activity on genes

Published OnlineFirst November 24, 2009; DOI: 10.1158/1535-7163.MCT-09-0479

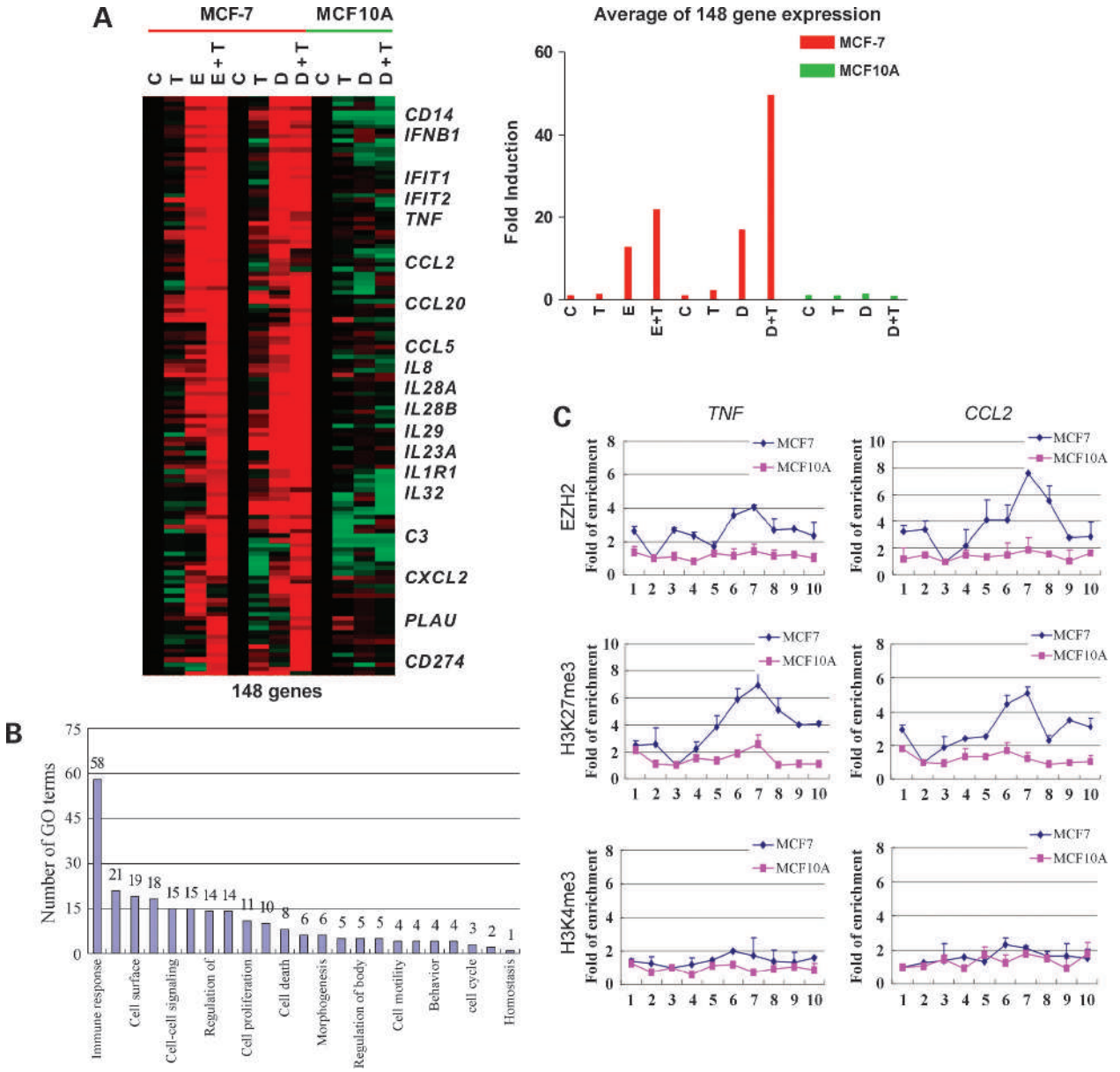

Figure 6. EZH2-repressed genes activated by DZNep alone or in synergy with TSA in cancer-specific manner. **A,** gene cluster diagram showing the expression profiles of 148 genes that are induced by either EZH2 siRNA (*E*) or DZNep (*D*) with or without cotreatment with TSA (*T*) in MCF-7 but not in MCF10A cells. *Right,* the fold induction under these conditions. **B,** Gene Ontology analysis reveals that 58 (including *TNF* and *CCL2*) of 148 genes were remarkably enriched for their roles in immune response. **C,** ChIP analysis indicates that EZH2 and H3K27me3 at *TNF* and *CCL2* locus are highly enriched in MCF-7 cells but not in MCF10A cells. The value that is <2 is classified as the baseline.

silenced by DNA methylation (21, 22). Instead, it strongly induces genes whose silencing is associated with EZH2-H3K27me3 (9, 22). This feature makes DZNep as a powerful agent in probing epigenetic process. Using DZNep in combination with other chromatin remodeling compounds (TSA and AZA), we were able to investigate multiple epigenetic mechanisms operating in cancer. First of all, the microarray analysis identified a set of 372 genes whose repression is effectively relieved by DZNep-related treatments in MCF-7 cells. Three distinct expression response patterns induced by different treatment conditions reflect three models of epigenetic mechanisms involving histone modifications. Further coupled with ChIP analysis of histone marks and EZH2 knockdown, we were able to nominate EZH2 target genes that are repressed by EZH2-H3K27me3 alone, or in coordination with histone deacetylation in breast cancer, which is consistent with our previous study in colon cancer (9). Furthermore, a small set of genes, such as *GAGEs* in MCF-7 cells, seems to be silenced by a mechanism involving the coordination between DNA methylation and histone

Published OnlineFirst November 24, 2009; DOI: 10.1158/1535-7163.MCT-09-0479

modifications. These results systematically show the complexity of epigenetic regulation in cancer beyond DNA methylation. Our data supports recent models that DNA methylation and EZH2-mediated gene silencing in principle target different set of genes in cancer cells (10, 27). Although both DNA methylation and H3K27me3 are detected at *GAGE2* in MCF-7 cells, we found that H3K27me3 was weakly enriched in a less methylated region of DNA and thus also contributes to gene repression. This result also highlights the heterogeneity of epigenetic mechanisms in breast cancer.

As one of cancer antigens, members of *GAGE* family are expressed in a wide variety of malignancies but generally not in normal tissues (37), a feature that warrants the development of *GAGE*-targeted cancer immunotherapy. Indeed, *GAGEs* were silenced in noncancerous human mammary epithelial cell line MCF10A, but showed varied expression levels in different breast cancer cell lines: namely, they were highly expressed in BT-474 cells, silenced in MCF-7 cells and basally in SK-BR-3 cells. This result is consistent with a recent report showing different *GAGE* protein expression levels owing to the cellular heterogeneity in malignancies (34). The data suggest that lack of *GAGE* expression in a subset of cancer cells within *GAGE*-positive tumors may result in failure of the development of *GAGE*-targeted cancer therapy. The distinct epigenetic mechanism involved in the silencing of *GAGE2* in different breast cancer cell lines suggests that different pharmacologic approaches are required for its reactivation. We showed that our combinatory pharmacologic approaches targeting different epigenetic components were able to translate all *GAGE*-negative cancer cells to *GAGE*-positive cancer cells. Importantly, because the enrichment of H3K27me3 at *GAGE2* locus is a cancer-specific event, the combination treatment does not seem to induce *GAGE2* expression in noncancerous MCF10A cells, thus possibly avoiding DZNep-related side effect on normal cells. We hypothesize that the overall activation of *GAGE* family by our approach may have implications in clinical immunotherapy for breast cancer.

We showed that perturbation of EZH2 function in MCF-7 cells through either pharmacologic inhibition or genetic deletion activated a prominent set of genes in inflammation and immunity network. This result raises the question of whether this effect may be detrimental to the efficacy of EZH2-targeted strategy or in fact provide an additional benefit. Accumulating literatures have highlighted the dilemmatic roles of inflammation and immunity network in cancer development, driving cancer progression or inhibiting tumor growth (38, 39). Contrary to the traditional view of chronic inflammation promoting cancer progression, recent evidences show that immune mediators such as *IL8* and CXCR2 (its associated ligands) have roles in implementing oncogene-induced senescence in cancer cells in autocrine and cell-autonomous fashion, a first-line defense against potentially dangerous mutations (40, 41). In addition, the local production of chemokines such as *CCL2* and *CXCL2* can attract tumor-infiltrating leukocytes to inhibit tumor growth in some instances (42). Thus, depending on the context, specific cytokines and chemokines elicit antitumorigenic or protumorigenetic effect, thereby affecting cancer immunity. In fact, 58 EZH2-repressed immunoresponse genes were reactivated by our pharmacologic approach in a cell-autonomous fashion, closely resembling what occurs with oncogene-induced senescence. We therefore speculate that EZH2 inhibition–mediated activation of human tumor–associated antigens (*GAGEs*) and other immune mediators might provide a protective host response to malignancy indirectly through the activation of innate immunity. However, a further study to validate this hypothesis using appropriate animal models is required. Hence, the development of clinical trials with EZH2-targeted therapeutic agents should proceed with caution and be mindful of the impact on other signaling cascades that may promote or antagonize its antitumor effect.

In summary, this study provides a comprehensive view of epigenetic mechanisms involving EZH2-mediated gene repression. The coordinated actions of EZH2 with other epigenetic components highlight the mechanistic heterogeneity, either among different genes in single cell line or the same genes in different cell contexts. In addition to yielding novel insights into epigenetic regulation, our study suggests that the best hope for epigenetic therapy may lie in the development of combinatory approach that targets multiple regulatory components or mechanisms rather than individual gene element.

Disclosure of Potential Conflicts of Interest

No potential conflicts of interest were disclosed.

Acknowledgments

We thank Li Zhuang for technical support in microarray hybridization.

References

1. Baylin SB, Ohm JE. Epigenetic gene silencing in cancer—a mechanism for early oncogenic pathway addiction? Nat Rev Cancer 2006;6:107–16.

2. Jones PA, Baylin SB. The fundamental role of epigenetic events in cancer. Nat Rev Genet 2002;3:415–28.

3. Cao R, Wang L, Wang H, et al. Role of histone H3 lysine 27 methylation in Polycomb-group silencing. Science 2002;298:1039–43.

4. Kirmizis A, Bartley SM, Kuzmichev A, et al. Silencing of human polycomb target genes is associated with methylation of histone H3 Lys 27. Genes Dev 2004;18:1592–605.

5. Bernstein BE, Mikkelsen TS, Xie X, et al. A bivalent chromatin structure marks key developmental genes in embryonic stem cells. Cell 2006;125:315–26.

6. Bracken AP, Dietrich N, Pasini D, Hansen KH, Helin K. Genome-wide mapping of Polycomb target genes unravels their roles in cell fate transitions. Genes Dev 2006;20:1123–36.

7. Varambally S, Dhanasekaran SM, Zhou M, et al. The polycomb group protein EZH2 is involved in progression of prostate cancer. Nature 2002;419:624–9.

8. Bracken AP, Pasini D, Capra M, et al. EZH2 is downstream of the pRB-E2F pathway, essential for proliferation and amplified in cancer. EMBO J 2003;22:5323–35.

9. Jiang X, Tan J, Li J, et al. DACT3 is an epigenetic regulator of Wnt/β-catenin signaling in colorectal cancer and is a therapeutic target of histone modifications. Cancer Cell 2008;13:529–41.

10. Kondo Y, Shen L, Cheng AS, et al. Gene silencing in cancer by histone

Published OnlineFirst November 24, 2009; DOI: 10.1158/1535-7163.MCT-09-0479

H3 lysine 27 trimethylation independent of promoter DNA methylation. Nat Genet 2008;40:741–50.

11. Fuks F. DNA methylation and histone modifications: teaming up to silence genes. Curr Opin Genet Dev 2005;15:490–5.

12. Vaissiere T, Sawan C, Herceg Z. Epigenetic interplay between histone modifications and DNA methylation in gene silencing. Mutat Res 2008; 659:40–8.

13. Dobosy JR, Selker EU. Emerging connections between DNA methylation and histone acetylation. Cell Mol Life Sci 2001;58:721–7.

14. Vire E, Brenner C, Deplus R, et al. The Polycomb group protein EZH2 directly controls DNA methylation. Nature 2006;439:871–4.

15. Wilson VL, Jones PA, Momparler RL. Inhibition of DNA methylation in L1210 leukemic cells by 5-aza-2′-deoxycytidine as a possible mechanism of chemotherapeutic action. Cancer Res 1983;43:3493–6.

16. Bender CM, Pao MM, Jones PA. Inhibition of DNA methylation by 5-aza-2′-deoxycytidine suppresses the growth of human tumor cell lines. Cancer Res 1998;58:95–101.

17. Nervi C, Borello U, Fazi F, et al. Inhibition of histone deacetylase activity by trichostatin A modulates gene expression during mouse embryogenesis without apparent toxicity. Cancer Res 2001;61:1247–9.

18. Suzuki H, Gabrielson E, Chen W, et al. A genomic screen for genes upregulated by demethylation and histone deacetylase inhibition in human colorectal cancer. Nat Genet 2002;31:141–9.

19. McGarvey KM, Fahrner JA, Greene E, et al. Silenced tumor suppressor genes reactivated by DNA demethylation do not return to a fully euchromatic chromatin state. Cancer Res 2006;66:3541–9.

20. Egger G, Aparicio AM, Escobar SG, Jones PA. Inhibition of histone deacetylation does not block resilencing of p16 after 5-aza-2′-deoxycytidine treatment. Cancer Res 2007;67:346–53.

21. Miranda TB, Cortez CC, Yoo CB, et al. DZNep is a global histone methylation inhibitor that reactivates developmental genes not silenced by DNA methylation. Mol Cancer Ther 2009;8:1579–88.

22. Tan J, Yang X, Zhuang L, et al. Pharmacologic disruption of Polycomb-repressive complex 2-mediated gene repression selectively induces apoptosis in cancer cells. Genes Dev 2007;21:1050–63.

23. Yu Q, La Rose J, Zhang H, et al. UCN-01 inhibits p53 up-regulation and abrogates γ-radiation-induced G(2)-M checkpoint independently of p53 by targeting both of the checkpoint kinases, Chk2 and Chk1. Cancer Res 2002;62:5743–8.

24. Yoshikawa H, Matsubara K, Qian GS, et al. SOCS-1, a negative regulator of the JAK/STAT pathway, is silenced by methylation in human hepatocellular carcinoma and shows growth-suppression activity. Nat Genet 2001;28:29–35.

25. Zhao Y, Tan J, Zhuang L, et al. Inhibitors of histone deacetylases target the Rb-E2F1 pathway for apoptosis induction through activation of proapoptotic protein Bim. Proc Natl Acad Sci U S A 2005;102: 16090–5.

26. Cheng JC, Yoo CB, Weisenberger DJ, et al. Preferential response of cancer cells to zebularine. Cancer Cell 2004;6:151–8.

27. Gal-Yam EN, Egger G, Iniguez L, et al. Frequent switching of Polycomb repressive marks and DNA hypermethylation in the PC3 prostate cancer cell line. Proc Natl Acad Sci U S A 2008;105:12979–84.

28. Heller G, Schmidt WM, Ziegler B, et al. Genome-wide transcriptional response to 5-aza-2′-deoxycytidine and trichostatin a in multiple myeloma cells. Cancer Res 2008;68:44–54.

29. Cameron EE, Bachman KE, Myohanen S, Herman JG, Baylin SB. Synergy of demethylation and histone deacetylase inhibition in the re-expression of genes silenced in cancer. Nat Genet 1999;21:103–7.

30. Hellebrekers DM, Melotte V, Vire E, et al. Identification of epigenetically silenced genes in tumor endothelial cells. Cancer Res 2007;67: 4138–48.

31. De Smet C, De Backer O, Faraoni I, et al. The activation of human gene MAGE-1 in tumor cells is correlated with genome-wide demethylation. Proc Natl Acad Sci U S A 1996;93:7149–53.

32. Yu J, Yu J, Rhodes DR, et al. A polycomb repression signature in metastatic prostate cancer predicts cancer outcome. Cancer Res 2007;67: 10657–63.

33. Zhao XD, Han X, Chew JL, et al. Whole-genome mapping of histone H3 Lys4 and 27 trimethylations reveals distinct genomic compartments in human embryonic stem cells. Cell Stem Cell 2007;1:286–98.

34. Gjerstorff MF, Johansen LE, Nielsen O, Kock K, Ditzel HJ. Restriction of GAGE protein expression to subpopulations of cancer cells is independent of genotype and may limit the use of GAGE proteins as targets for cancer immunotherapy. Br J Cancer 2006;94:1864–73.

35. De Backer O, Arden KC, Boretti M, et al. Characterization of the GAGE genes that are expressed in various human cancers and in normal testis. Cancer Res 1999;59:3157–65.

36. Glazer RI, Knode MC, Tseng CK, Haines DR, Marquez VE. 3-Deazaneplanocin A: a new inhibitor of S-adenosylhomocysteine synthesis and its effects in human colon carcinoma cells. Biochem Pharmacol 1986;35:4523–7.

37. Scanlan MJ, Gure AO, Jungbluth AA, Old LJ, Chen YT. Cancer/testis antigens: an expanding family of targets for cancer immunotherapy. Immunol Rev 2002;188:22–32.

38. Hagemann T, Balkwill F, Lawrence T. Inflammation and cancer: a double-edged sword. Cancer Cell 2007;12:300–1.

39. Mantovani A, Allavena P, Sica A, Balkwill F. Cancer-related inflammation. Nature 2008;454:436–44.

40. Acosta JC, O'Loghlen A, Banito A, et al. Chemokine signaling via the CXCR2 receptor reinforces senescence. Cell 2008;133:1006–18.

41. Kuilman T, Michaloglou C, Vredeveld LC, et al. Oncogene-induced senescence relayed by an interleukin-dependent inflammatory network. Cell 2008;133:1019–31.

42. Balkwill F. Cancer and the chemokine network. Nat Rev Cancer 2004; 4:540–50.

AACR American Association for Cancer Research

Molecular Cancer Therapeutics

Combinatorial pharmacologic approaches target EZH2-mediated gene repression in breast cancer cells

Feng Sun, Eli Chan, Zhenlong Wu, et al.

Mol Cancer Ther 2009;8:3191-3202. Published OnlineFirst November 24, 2009.